Spectrochimica Acta Part A: Molecular and Biomolecular Spectroscopy 146 (2015) 331–341

Contents lists available at ScienceDirect

Spectrochimica Acta Part A: Molecular and Biomolecular Spectroscopy

journal homepage: www.elsevier.com/locate/saa

Effect of annealing on the luminescence properties of YVO_4:Dy^{3+} phosphor on co-doping Pb^{2+} ions

Ch. Victory Devi [a], N. Rajmuhon Singh [b,*]

[a] Department of Chemistry, Pachhunga University College, Aizawl 796 001, Mizoram, India
[b] Department of Chemistry, Manipur University, Canchipur, 795003 Imphal, India

HIGHLIGHTS

- Single tetragonal phase.
- Emission of white light on co-doping Pb^{2+}.
- Maximum emission under 280 nm excitation wavelength.
- Independent of emission color on excitation wavelength.
- Tuning of emission color on annealing.

GRAPHICAL ABSTRACT

CIE chromaticity of (a) as-prepared and (b) 900 °C annealed 1 at.% Pb^{2+} co-doped YVO_4:5Dy^{3+} nanoparticles under excitation wavelength at 280 nm.

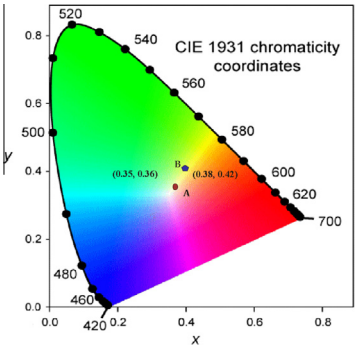

ARTICLE INFO

Article history:
Received 17 November 2014
Received in revised form 9 February 2015
Accepted 1 March 2015
Available online 9 March 2015

Keywords:
Single phase
Tunable
Annealing temperature
Potential phosphor

ABSTRACT

Pb^{2+} co-doped YVO_4:Dy^{3+} phosphors have been synthesized at a relatively low temperature of 120 °C via ethylene glycol route. The samples are further annealed at 500 and 900 °C. The prepared samples were characterized by XRD, SEM, spectra energy dispersive analysis of X-ray (EDAX) and photoluminescence spectroscopy. XRD patterns of all samples are well indexed with single tetragonal phase of YVO_4. The emission intensity of Dy^{3+} is significantly enhanced on co-doping Pb^{2+} ions. The highest emission is obtained at 7 at.% Pb^{2+} for 900 °C annealed samples. Both emission intensity and decay lifetime increases on annealing the samples from 500 to 900 °C. On co-doping Pb^{2+} into YVO_4:Dy^{3+} phosphors, the emission color falls near the white region and then shift towards yellow region on annealing from 500 to 900 °C thereby indicating that annealing temperature play a role on tuning the color of the phosphors. As well as the emission color of the phosphors remain the same even on changing the excitation wavelengths from 280 nm, which would serve as potential phosphors for white emission in LED applications.

Introduction

Nowadays white-light-emitting diodes (White LEDS) are considered as a promising new light emitting source for solid state lightening applications, for their advantages as a high luminescent efficiency, long lifetimes, low energy consumption and environmental friendly characteristics [1–5]. The development of White LEDs was first realized by combining a blue LED and a yellow

* Corresponding author. Tel.: +91 9436080780; fax: +91 3852435145.
E-mail addresses: victorychanambam@gmail.com (Ch. Victory Devi), rajmuhon@gmail.com (N. Rajmuhon Singh).

http://dx.doi.org/10.1016/j.saa.2015.03.039
1386-1425/

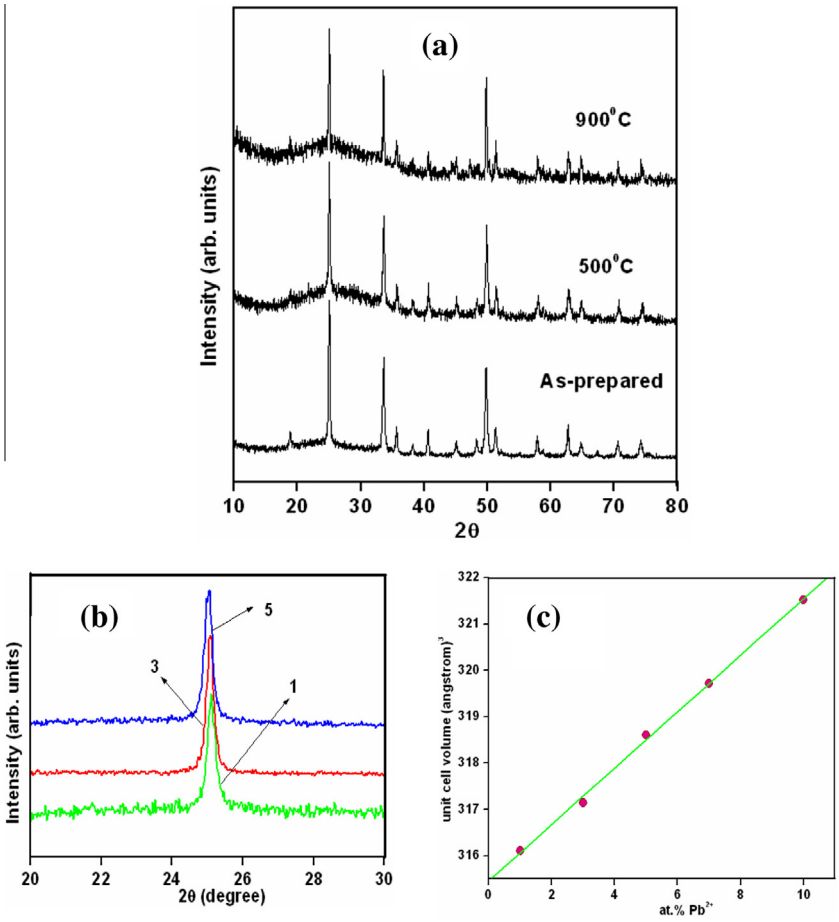

Fig. 1. (a) XRD pattern of as-prepared, 500 °C annealed and 900 °C annealed YVO_4:5Dy^{3+}, 5Pb^{2+}; (b) shift in the diffraction peaks for YVO_4 after co-doping Pb^{2+} and (c) plot of unit cell volume with Pb^{2+} concentration for as-prepared samples.

phosphor $(Y, Ga)_3(Al, Ga)_5O_{12}:Ce^{3+}$. The other approaches consisting of assembling red, green and blue LEDs in one device or by combining a near UV LED chip (370–410) with red, green and blue phosphors were also used for white LEDs. However, such LEDs have lower efficiency, short lifetime, instability and poor color rendering index. These drawbacks can be overcome by using a UV chip with primary emission of 370–410 nm instead of blue LED [6–8]. That is, the UV chip is used as excitation light. Therefore, the near UV chip with excitable phosphors is another attractive combination for white light generation. Recently, white LEDs fabricated using near ultraviolet LED or ultraviolet (UV) LED with single host emission color-tunable phosphor have been investigated to improve the color-rendering index and to tune the correlated color temperature by systematically tuning the relative dopant content to sensitizer and activator. A single-phase white light phosphor is produced by co-doping sensitizer and activator into the same host matrix, using the principle of energy transfer from sensitizer to activator. For instance, $Ba_{1.3}Ca_{0.7}SiO_4:Eu^{2+}$–$Mn^{2+}$ [9], $BaMgP_2O_7:Eu^{2+}$–Mn^{2+} [10] and $Ca_9A(PO_4)_7:Eu^{2+}$, Mn^{2+} (A = Y, La, Gd) [11–13] are reported to be the white emitter phosphors. Very recently, white light emitting $Lu_6O_5F_8$:20% Yb^{3+}, 1% Er^{3+} (Tm^{3+}) nanoparticles co-doped with Li^+ have been reported [14]. As a continuation of the approach towards the development of white LEDs we attempt to synthesize the Pb^{2+} co-doped YVO_4:5Dy^{3+} phosphors in the present work. The transition metal Pb^{2+} has $6s^2$ configuration and Pb^{2+} is a more active metal so 6s electron can be easily excited to harvest the near-UV light or transfer to the empty d-orbital of V^{5+} [15].

YVO_4, having a zircon-typed tetragonal structure is one of the most promising inorganic luminescent materials because of their wide practical application in many display devices [16–21]. Doping of Ln^{3+} ions into YVO_4 produce high luminescencent performance owing to abundant emission colors basing mainly on *f–f* transitions [22,23]. Dy^{3+} is a well-known good activator exhibiting three visible emission bands including blue emission at 480 nm, yellow emission at 576 nm and feeble red emission at 660 nm [24–26]. The hypersensitive transition of Dy^{3+} ions can be easily influenced by micrographic environment, so Dy^{3+} doped YVO_4 will be a potential white phosphor on co-doping with Pb^{2+}. So, to the best of our knowledge, Pb^{2+} co-doped $YVO_4:Dy^{3+}$ prepared via ethylene glycol route employing low temperature, ~120 °C has not been reported so far. In the present study, Pb^{2+} co-doped YVO_4:5Dy^{3+} have been successfully synthesized via a simple co-precipitation method. The co-doping effect of Pb^{2+} and annealing temperatures on the photoluminescence of YVO_4:5Dy^{3+} has been studied in detailed. The investigation on white emission of the synthesized phosphor was mainly focused in the present paper.

Experimental

Materials and synthesis

$Y_2(CO_3)_3$, $Dy(CH_3COO)_3$, NH_4VO_3 and $Pb(NO_3)_2$ were used as source materials in the present study. Pb^{2+} co-doped YVO_4:5Dy^{3+} phosphors were synthesized by co-precipitation method via

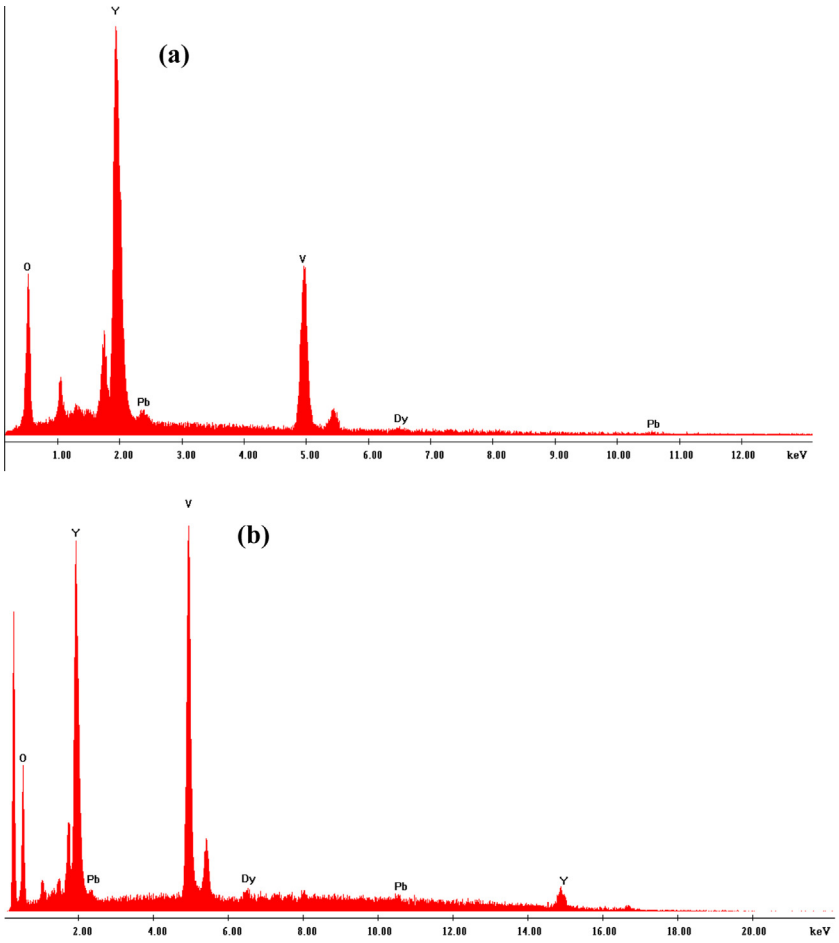

Fig. 2. EDX spectra of (a) 500 °C annealed and (b) 900 °C annealed YVO_4:$5Dy^{3+}$, $5Pb^{2+}$ nanoparticles.

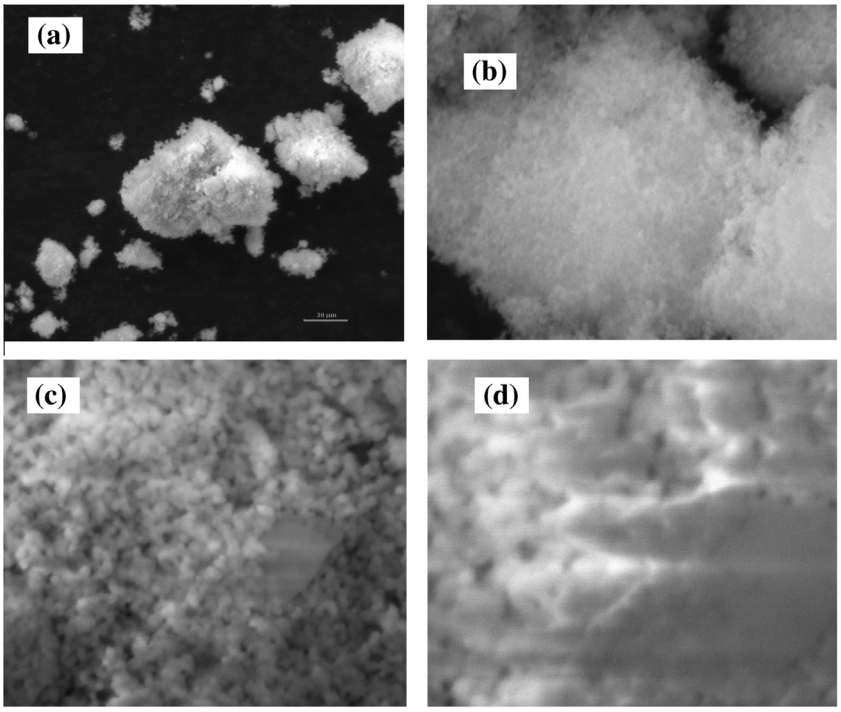

Fig. 3. SEM images of 500 °C annealed YVO_4:$5Dy^{3+}$, $5Pb^{2+}$ (a) at low magnification and (b) at high magnification, and those annealed at 900 °C (c) at low magnification and (d) at high magnification.

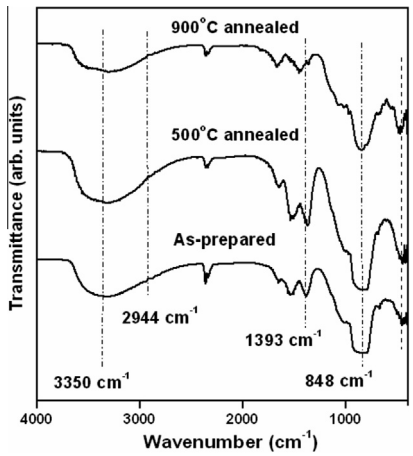

Fig. 4. FT-IR spectra of as-prepared, 500 and 900 °C annealed YVO_4:5Dy^{3+}, Pb^{2+} (5 at.%) nanoparticles.

ethylene glycol route employing a very low temperature of 120 °C. In a typical preparation of 3 at.% Pb^{2+} co-doped YVO_4:5Dy^{3+} nanoparticles, 0.25 g of $Y_2(CO_3)_3$, 0.025 g of $Dy(CH_3COO)_3$ and 0.03 g of $Pb(NO_3)_2$ were dissolved together in concentrated nitric acid (HNO_3) in a 250 ml round bottom flask and then heated with addition of double distilled water at least five times in order to remove the excess acid. To this, 0.1777 g of NH_4VO_3 and 25 ml of ethylene glycol (EG) were added. Then, the solution was stirred for uniform mixing. NaOH was used as a precipitating agent to control the pH of the mixture. The reaction mixture was then heated at ~120 °C for 3 h under refluxing condition until the white precipitation is completed.

The precipitate so obtained was allowed to cool at room temperature and then washed three times by centrifugation in ethanol and then acetone to remove the excess of EG, and then dried at room temperature for four days. Finally, the as-prepared samples were annealed at 500 and 900 °C for 3 h to analyze their photoluminescence properties in detail.

Measurement and characterization

The crystal structure of all the samples were characterized by X-ray powder diffraction (XRD) analysis using PANalytical powder diffractometer (X'Pert PRO) with Cu$K\alpha$ (1.5405 Å) radiation with Ni filter. The particle morphologies and elemental composition were examined by SEM using FEI Quanta 250 equipped with an energy dispersive X-ray spectroscopy. Fourier transform infrared (FTIR) spectra were measured on a Shimadzu (8400S) using a KBr pellet technique. The photoluminescence spectra and decay curves were measured by Perkin Elmer (LS-55), which is composed of a 20 kW Xe discharge lamp, for 8 μs duration, as the excitation source having pulse width at half height <10 μs. All the measurements were carried out at room temperature.

Results and discussions

XRD

The XRD pattern of all the prepared YVO_4:5Dy^{3+}, xPb^{2+} (x = 0, 1, 3, 5, 7 and 10) samples are indexed well with single tetragonal phase of YVO_4 having space group $I4_1/amd$ (JCPDS 17-0341). No

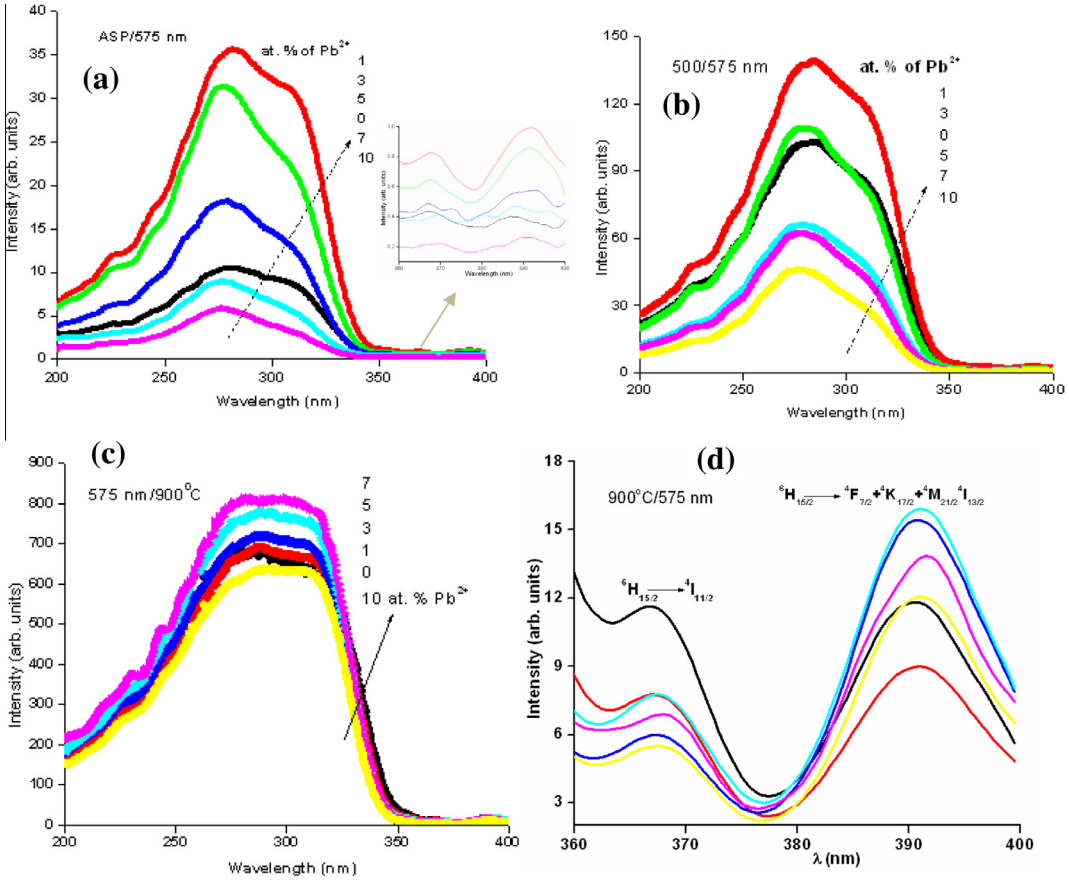

Fig. 5. Excitation spectra of (a) as-prepared (b) 500 and (c) 900 °C annealed Pb^{2+} co-doped YVO_4:5Dy^{3+} nanoparticles (Pb = 0, 1, 3, 5, 7 and 10 at.%) on monitoring emission wavelength at 575 nm. (d) Expanded excitation spectra of 900 °C annealed samples.

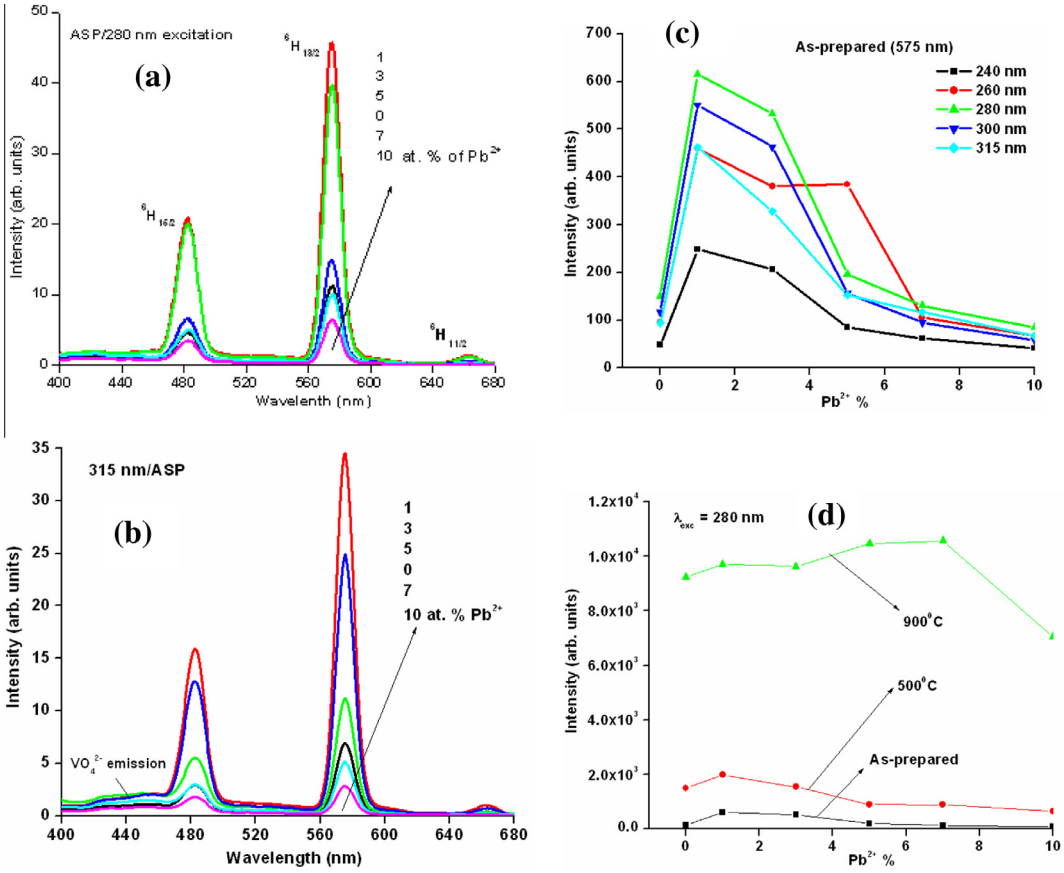

Fig. 6. Emission spectra of as-prepared Pb^{2+} co-doped YVO_4:$5Dy^{3+}$ nanoparticles (Pb^{2+} = 0, 1, 3, 5, 7 and 10 at.%) under excitation wavelength at (a) 280 nm and (b) 315 nm. (c) Plot of integrated area vs concentration of Pb^{2+} for as-prepared at different excitation wavelengths. (d) Plot of integrated area vs concentration of Pb^{2+} for as-prepared, 500 and 900 °C annealed samples under excitation 280 nm.

secondary phases are observed indicating the formation of a pure tetragonal phase indicating that the Pb^{2+} is quantitatively substituted into the lattice sites of Y^{3+}. Fig. 1a shows the typical XRD pattern of as-prepared, 500 and 900 °C annealed $5Pb^{2+}$ co-doped YVO_4:$5Dy^{3+}$. From Fig. 1a, we see that tetragonal crystal phase remain the same in both 500 and 900 °C annealed samples. On annealing the samples at 500 and 900 °C, the width of the peak decreased and become sharp with increased intensity suggesting the improved crystallinity of the samples due to increase in particle size.

The diffraction peaks of YVO_4 shift towards lower 2θ on co-doping Pb^{2+} ions. This is related to the small size of Y^{3+} (1.019 Å) as compared to Pb^{2+} (1.35 Å). And that of Dy^{3+} is 1.027 (Å). The shifting of diffraction peak is shown from 20° to 30° in Fig. 1b. It suggests that Pb^{2+} occupies the lattice sites of Y^{3+}. So the volume expansion occurs on increasing the concentration of Pb^{2+} (Fig. 1c).

The average crystallize size of the particles were calculated from intense diffraction peak (200) using Debye's formula:

$$D = 0.9\lambda/\beta\cos\theta \quad (1)$$

where λ is the X-ray wavelength used, θ is the diffraction angle of the diffraction peak (200), and β is defined as the half width after subtracting instrumental broadening. The average crystallize sizes of 5 at.% Pb^{2+} co-doped as-prepared, 500 and 900 °C annealed samples are found to be ~34, 50 and 85 nm, respectively. The samples show high crystallinity and intensity increase with Pb^{2+} concentration. Also annealed samples at 500 and 900 °C show the increase in crystalline nature.

EDX

We have analyzed the EDX spectra of as-prepared, 500 and 900 °C heated samples to study the expected elemental composition of Pb^{2+} co-doped YVO_4:Dy^{3+}. Fig. 2a and b shows the EDX spectra of 500 and 900 °C annealed 5 at.% Pb^{2+} co-doped YVO_4:$5Dy^{3+}$ phosphors. It is seen from analyzed result, that the EDAX spectra of 500 and 900 °C annealed 5 at.% Pb^{2+} co-doped YVO_4:Dy^{3+} as presented in Fig. 2a and b exhibits not only Y, V, Dy signals but also the Pb which indicates the incorporation of Pb^{2+} in the YVO_4:Dy^{3+} nanocrystals. Neither Na or C signals were detected in the EDAX spectrum taken for the as-prepared (Fig. S1a), 500 and 900 °C annealed 5 at.% Pb^{2+} co-doped YVO_4 which means that the products are free from NaOH and carbonates. 500 °C annealed samples give the composition in at.%: O = 80.95; Y = 12.45; V = 6.24; Dy = 0.20; Pb = l.17 and 900 °C annealed sample give the composition in at.%: O = 64.60; Y = 11.93; V = 22.06; Dy = 1.14 and Pb = 0.27. The amount of V^{5+} is found to be increased on annealing the samples to 900 °C. As-prepared sample is also found to have the composition: O = 79.96; Y = 13.1; V = 6.53; Dy = 0.26 and Pb = 0.26.

SEM study

The morphology of the prepared samples was investigated by SEM observations. Fig. 3a–d shows the SEM images of 500 and 900 °C heated YVO_4:$5Dy^{3+}$, $5Pb^{2+}$ phosphors. SEM image of as-prepared samples was also shown in Fig. S1b. From the low

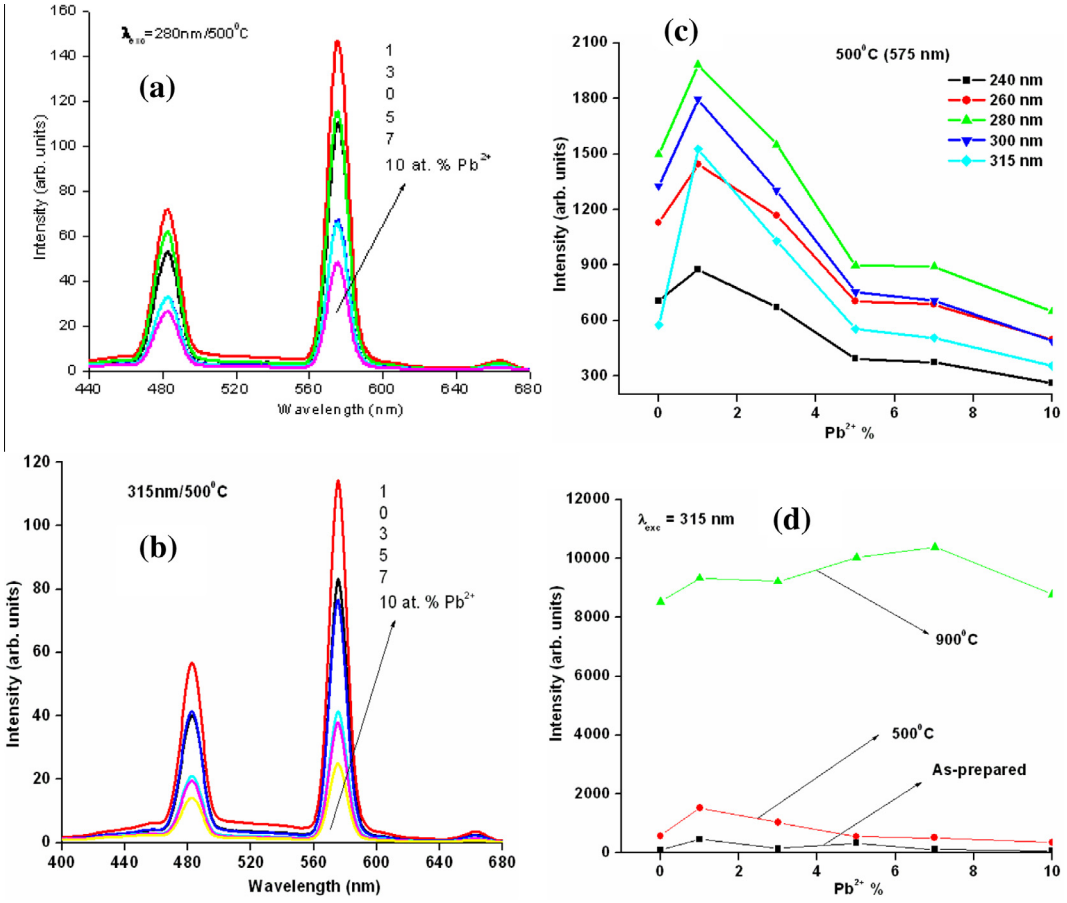

Fig. 7. Emission spectra of 500 °C annealed Pb^{2+} co-doped YVO_4:5Dy^{3+} nanoparticles (Pb = 0, 1, 3, 5, 7 and 10 at.%) under excitation wavelength at (a) 280 nm and (b) 315 nm. (c) Plot of integrated area vs concentration of Pb^{2+} for 500 °C annealed at different excitation wavelengths. (d) Plot of integrated area vs concentration of Pb^{2+} for as-prepared, 500 and 900 °C annealed samples under excitation wavelength 315 nm.

and high magnification SEM images of Fig. 3(a) and (b) it can be seen that particles have non-uniform surface without any agglomeration with lengths of 5–10 μm. SEM image of those of 900 °C annealed samples shows spherical shape but it seems that crystallization process starts as there is a large size particle in the image. However, High magnification SEM images revealed spindle like shape with a diameter of about 1 μm.

FT-IR spectra study

The measured IR spectra of as-prepared, 500 and 900 °C annealed samples were shown in Fig. 4. The peaks around 450 and 848 cm^{-1} correspond to the vibrations of Y–O [27] and V–O (from VO_4^{3-} group) [28] bonds respectively which became much more prominent in 900 °C annealed samples. The broad peak around 3350 cm^{-1} and weak band at 1647 cm^{-1} are attributed to stretching and bending vibrations of O–H group, respectively [29]. These two bands are due to the water absorbed on the surface of the samples. The band at 2944 cm^{-1} are assigned to CH_2 stretching vibrations of EG molecules present on the surface of the nanoparticles [30]. Peaks around 1021 and 1393 cm^{-1} are related to V=O and C–O bonds, respectively [31]. The pronounced vibration bands of Y–O and V–O bonds on annealing the samples demonstrate the formation of crystalline YVO_4 nanocrystal agreeing well with result of XRD. And the peak around 2944 cm^{-1} disappeared and the absorption bands of O–H stretching also decreases, that is, the presence of organic impurity such as O–H, CH_2 in the samples are reduced on heat treatment, thereby increasing crystalline nature of the particle.

Photoluminescence study

Fig. 5a–c shows the excitation spectra of as-prepared, 500 and 900 °C annealed Pb^{2+} co-doped YVO_4:5Dy^{3+} nanoparticles obtained on monitoring emission wavelength at 575 nm. The excitation spectrum consists of a broad band ranging from 210 to 330 nm with a maximum at 280 nm and shoulder at 315 nm. It is well known that band edge 315 excitation is due to the charge transfer from oxygen ligands to the central vanadium atom inside the VO_4^{3-} absorption. The short wavelength 280 nm excitation is assigned to the overlap of VO_4^{3-} absorption and charge transfer transition between Dy^{3+} and O^{2-} [31,32]. The appearance of a broad excitation band confirms the emission of Dy^{3+}occurs via energy transfers from excited VO_4^{3-}. Weaker excitation bands appeared in longer wavelength was due to 4*f*–4*f* transitions of Dy^{3+} ions: 366 nm ($^6H_{15/2} \rightarrow {}^4I_{11/2}$) and 391 nm ($^6H_{15/2} \rightarrow {}^4F_{7/2} + {}^4K_{17/2} + {}^4M_{21/2} + {}^4I_{13/2}$) which became prominent on heat treatment of samples (Fig. 5d). However, the intensity of these 4*f*–4*f* transitions of Dy^{3+} is very weak as compared to the intensity from Dy–O and V–O absorption showing the transfer of excitation energy from either Dy–O or V–O CT to Dy^{3+}.

The intensity of excitation spectra are increased significantly on co-doping Pb^{2+} ions into YVO_4:5Dy^{3+}. However, the band edge excitation has not shifted towards longer wavelength at all. The

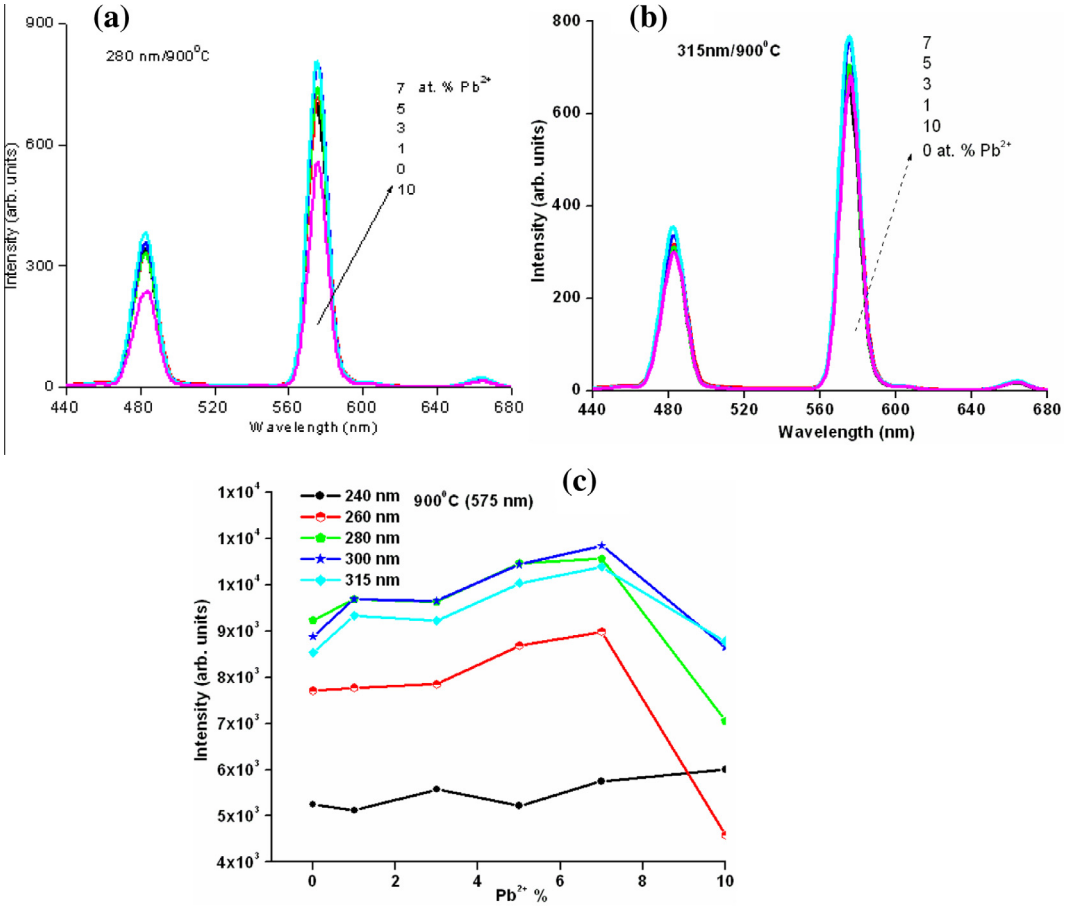

Fig. 8. Emission spectra of 900 °C annealed Pb^{2+} co-doped YVO_4:5Dy^{3+} nanoparticles (Pb = 0, 1, 3, 5, 7 and 10 at.%) under excitation wavelength at (a) 280 nm and (b) 315 nm. (c) Plot of integrated area vs concentration of Pb^{2+} for 500 °C annealed at different excitation wavelengths.

Pb^{2+} has $6s^2$ configuration; the 6s electron may be transfer to the empty d orbital of V^{5+} so, the energy levels of charge transfer from 6s electron of Pb^{2+} to the empty d orbital of V^{5+} must be enough to produce high luminescence efficiency. The intensity increases up to 1 at.% Pb^{2+} and then decreases on further addition of Pb^{2+} concentration. Beyond 1 at.% Pb^{2+}, the long wavelength C–T band diminishes in intensity and disappears completely when the concentration of Pb^{2+} ion is 10 at.%. However, the absorption in the short-wavelength (260–280 nm) seems to be increase gradually (Fig. 5a). On annealing the samples at 500 and 900 °C, the excitation intensity enhanced significantly. In case of 500 °C annealed samples, the trend of excitation spectra is quite similar to those of as-prepared samples although the intensity is increased. However, in 900 °C annealed samples, a broad intense excitation peak (Fig. 5c) is observed suggesting the efficient transfer of excitation energy from host/VO_4^{3-} to Dy^{3+}.

The emission spectra of Pb^{2+} co-doped YVO_4:5Dy^{3+} phosphors obtained under excitation of 280 and 315 nm are shown in Fig. 6a and b. We find main emission lines of Dy^{3+}, which consists of magnetic dipole transition $^4F_{9/2} \rightarrow {}^6H_{15/2}$ at 482 nm (blue), electric dipole transition $^4F_{9/2} \rightarrow {}^6H_{13/2}$ at 575 nm (yellow) and weak $^4F_{9/2} \rightarrow {}^6H_{11/2}$ transition at 668 nm (red) [33]. The emission spectra of YVO_4:5Dy^{3+}, Pb^{2+} under 240, 260 and 300 nm show similar behavior (Fig. S2a–c). The broad peak around 410–460 nm due to VO_4^{3-} emission is relatively low. On annealing the samples, the intensity of the broad peak around 410–460 nm decreases due to reduction in lattice defects and energy transfer from host/VO_4^{3-} to Dy^{3+} increases and then the emission intensity of Dy^{3+} are correspondingly increased.

The emission intensity of as-prepared samples are maximum under 280 nm excitation and then decreased in following order of 300, 315, 260 and 240 nm excitation (Fig. S3). On annealing the samples from 500 to 900 °C, the emission intensity of Dy^{3+} is still found to be highest under 280 nm excitation. This is due to the reduction of non-radiative transitions arising from O–H vibrations present on the surface of the samples. The variation in emission intensity under different excitation wavelength can be understood by calculating the integrated area after fitting the Gaussian distribution function, Eq. (2):

$$I = I_0 + \sum_{i=1}^{2} \frac{A_i}{w_i\sqrt{\pi/2}} e^{2(\lambda-\lambda_{ci})^2/w_i^2} \quad (2)$$

where I is the observed intensity, I_0 is the background intensity, w_i the FWHM of the curve, A_i the area under the curve, λ the wavelength and λ_{ci} the mean value corresponding to the transition. The fitting were carried out for $^4F_{9/2} \rightarrow {}^6H_{13/2}$ and $^6H_{15/2}$ in between 460 and 600 nm. The change in emission intensity of the $^4F_{9/2} \rightarrow {}^6H_{13/2}$ (575 nm) with Pb^{2+} concentration (Pb^{2+} = 0, 1, 3, 5, 7 and 10 at.%) at different excitation wavelengths is shown in Fig. 6c and that of $^4F_{9/2} \rightarrow {}^6H_{15/2}$ transition (482 nm) is also shown in Fig. S2d. The intensity increases up to 1 at.% Pb^{2+} and then decreases on increasing Pb^{2+} content. This is due to the well known luminescent quenching phenomena. On increasing Pb^{2+}

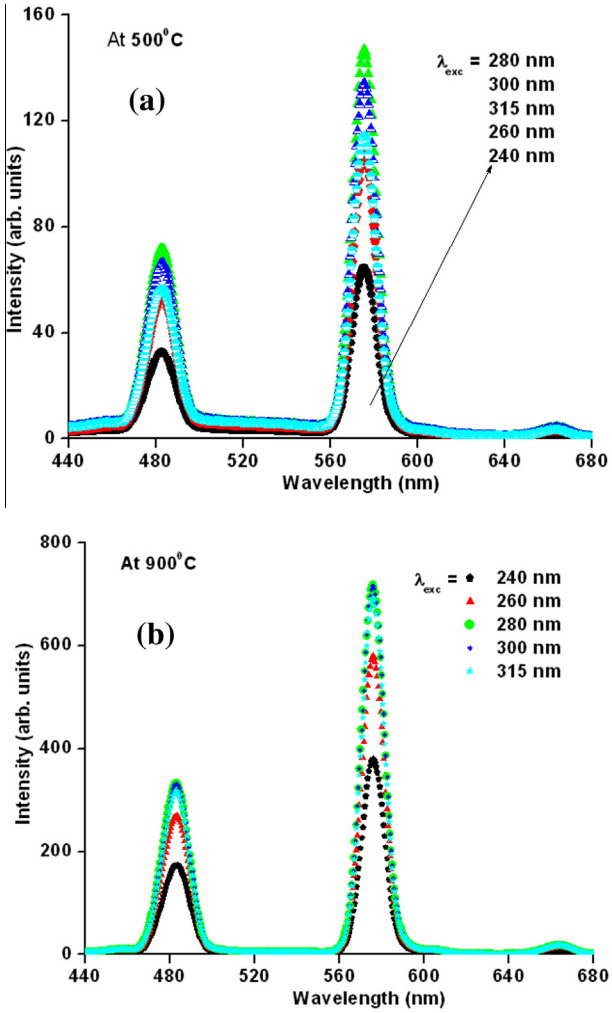

Fig. 9. Luminescence spectra of (a) 500 and (b) 900 °C annealed 1 at.% Pb^{2+} co-doped YVO_4:5Dy^{3+} nanoparticle at different excitation wavelengths.

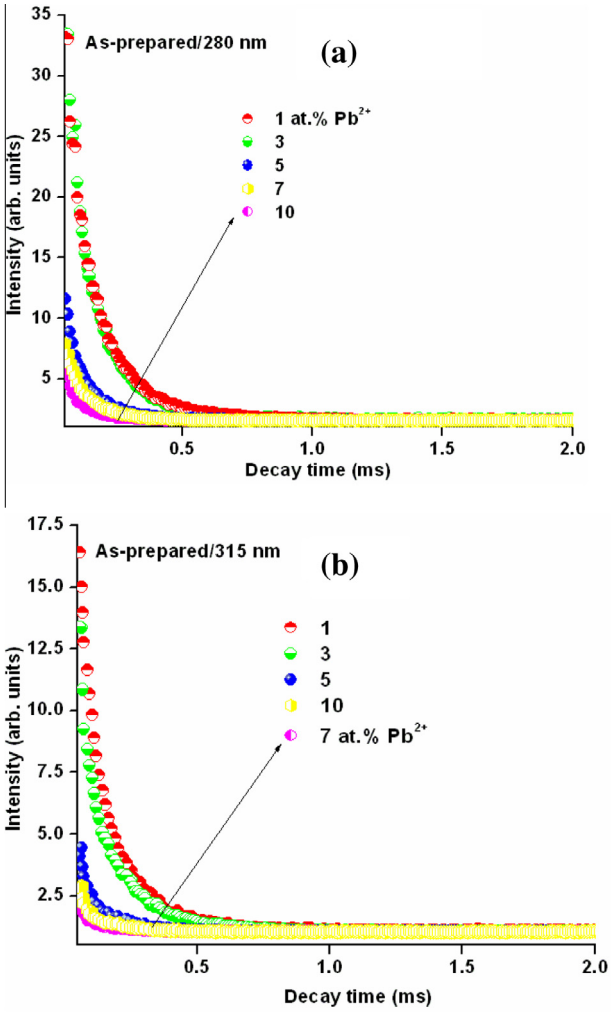

Fig. 10. Luminescence decay spectra of as-prepared Pb^{2+} co-doped YVO_4:5Dy^{3+} nanoparticles at 280 and 315 nm excitations.

concentration, energy may be lost to the quenching sites from electron migration among Pb^{2+} ions causing low emission of Dy^{3+}. Thus the optimum concentration for maximum emission is found to be 1 at.% Pb^{2+}. And the intensity of electric dipole transition is dominant over magnetic dipole transition in all emission spectra obtained under different excitation wavelengths. This can be explained as in crystalline YVO_4, Y^{3+} ions in distorted dodecahedral (eightfold) coordination are linked with eight neighboring O^{2-} ions (D_{2d} point symmetry of Y^{3+}, without inversion symmetry) and V^{5+} in the $[VO_4]^{3-}$ are tetrahedrally coordinated with O^{2-} ions. So, when doped Dy^{3+}/Pb^{2+} occupied the Y^{3+} sites, the non inversion center cause the domination of hypersensitive $^4F_{9/2} \rightarrow {}^6H_{13/2}$ transition over magnetic dipole transition $^4F_{9/2} \rightarrow {}^6H_{15/2}$. The hypersensitive transition $^4F_{9/2} \rightarrow {}^6H_{13/2}$ obeying the selection rule ($J = 2$) is very sensitive to the local environment whereas the magnetic dipole transition $^4F_{9/2} \rightarrow {}^6H_{15/2}$ hardly varies with the crystal field strength around Dy^{3+} ions. Most prominently $^4F_{9/2} \rightarrow {}^6H_{13/2}$ emission transition is dominant in its emission spectra when Dy^{3+} ion is located at low-symmetry local sites without non inversion centers [34]. The ratio between the electric dipole and magnetic dipole known as asymmetric ratio is a measure of the site symmetry in which the dysprosium ions are situated. The asymmetric ratio in the present case is found to be in the range of 1.8–3.0. The FWHM values of the Pb^{2+} co-doped ions are in the range of 10.8–11.3 and 12.6–13.1 for electric dipole and magnetic dipole transitions in Dy^{3+}. It gives enhanced integrated area under magnetic dipole transition and, thereby, the asymmetric ratio is not so high in present case.

Fig. 7a and b show the emission spectra of Pb^{2+} co-doped YVO_4:5Dy^{3+} annealed at 500 °C under excitation wavelengths at 280 and 315 nm. The emission spectra at 240, 260 and 300 nm excitation are shown in Fig. S4a–c. The integrated area under $^4F_{9/2} \rightarrow {}^6H_J$ ($J = 13/2$ and 15/2) decrease with increase of Pb^{2+} concentration, which are shown in Figs. 7c and S4c. The trend of decrease in emission intensity is slightly different as compared to as-prepared samples. However, the emission intensity is significantly improved by annealing at 500 °C, which is related to increase in crystallize size and also decrease in non-radiative processes.

The emission spectra of 900 °C annealed samples of Pb^{2+} co-doped YVO_4:5Dy^{3+} for 280 and 315 nm excitation are shown in Fig. 8a and b And that of emission spectra obtained under 240, 260 and 300 nm is also shown in Fig. S5a–c. It is observed that luminescence intensity is increased up to 7 at.% Pb^{2+} in all emission spectra and then decreases with further increase of Pb^{2+} contents except the emission under 240 nm excitation where the luminescence intensity is increased up to 10 at.% Pb^{2+}. The luminescence intensity of the 900 °C annealed sample is twenty times that of 500 °C annealed sample and 80 times that of the as-prepared

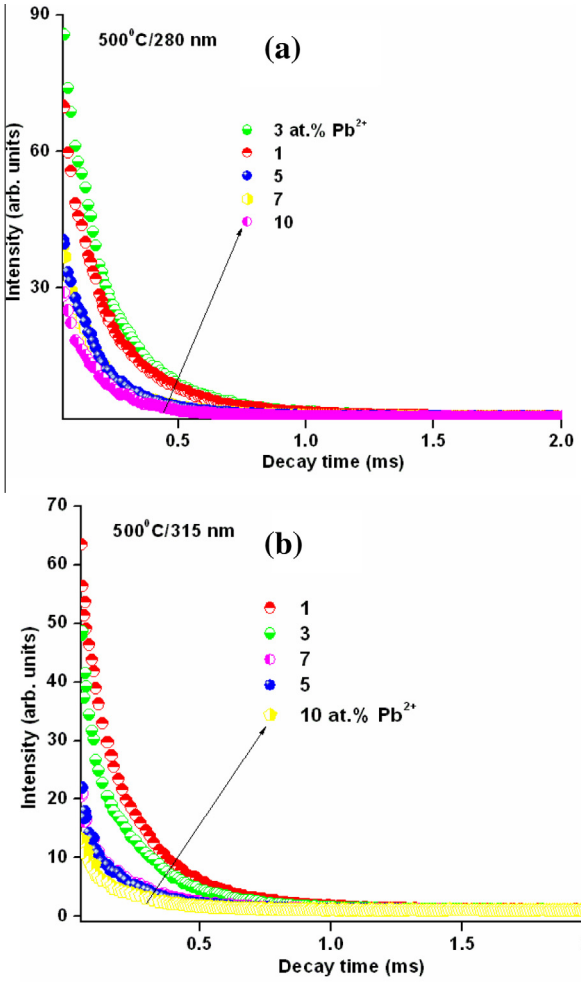

Fig. 11. Luminescence decay spectra of 500 °C annealed Pb^{2+} co-doped YVO_4:$5Dy^{3+}$ nanoparticles at 280 and 315 nm excitations.

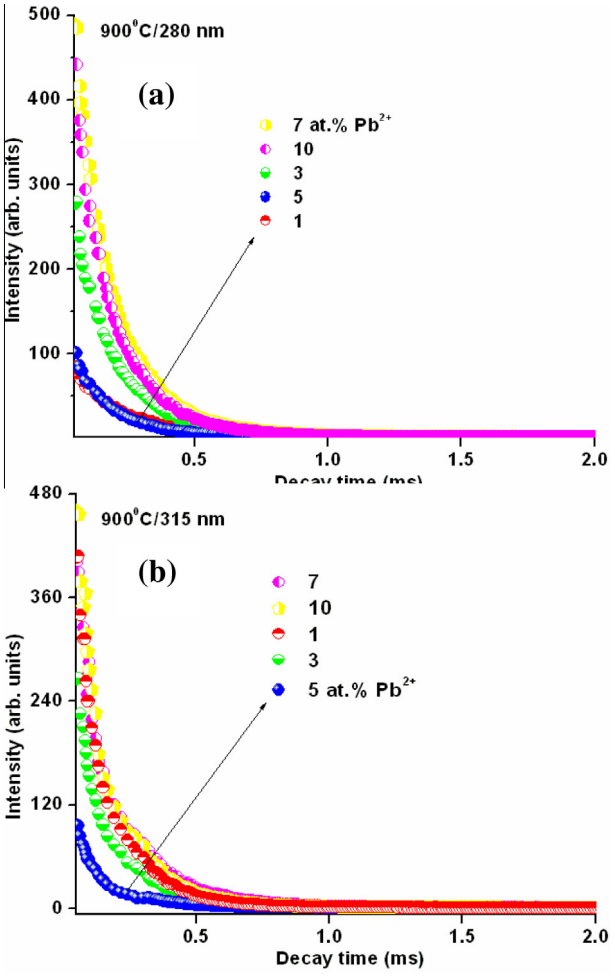

Fig. 12. Luminescence decay spectra of 900 °C annealed Pb^{2+} co-doped YVO_4:$5Dy^{3+}$ nanoparticles at 280 and 315 nm excitations.

sample (Fig. 9). As compared to as-prepared sample and 500 °C annealed samples, 900 °C annealed samples with 1–10 at.% Pb^{2+} concentration have high luminescence intensity. Improvement in luminescent intensity is due to the extent of reduction of non-radiative rate arising from O–H vibrations of water present on the surface of particles and decreased surface ratio on annealing at higher temperatures. It is clearly demonstrate that the luminescent intensity strongly depends on annealing temperatures.

Luminescence decay study

The kinetic decay curves of the level $^4F_{9/2}$ (575 nm) were measured for as-prepared, 500 and 900 °C annealed Pb^{2+} co-doped YVO_4:$5Dy^{3+}$ samples. Fig. 10a and b show the luminescence decay curves for $^4F_{9/2} \rightarrow {}^6H_{13/2}$ emission for prepared samples when excited at 280 and 315 nm. For annealed samples luminescence decay spectra were also shown in Figs. 11 and 12. All experimental decay curves are well fitted by bi-exponential decay equation,

$$I = I_1 e^{-t/\tau_1} + I_2 e^{-t/\tau_2} \quad (3)$$

where I_1 and I_2 are the intensities at different time intervals and τ_1 and τ_2 their corresponding lifetimes. Based on this, the average lifetime can be calculated using equation,

$$\tau_{av} = \frac{I_1\tau_1^2 + I_2\tau_2^2}{I_1\tau_1 + I_2\tau_2} \quad (4)$$

Bi-exponential fitting is observed when one of the following conditions happens:

(i) Difference in the non-radiative probability of decays for lanthanide ions at or near the surface and lanthanide ions in the core of the particles [35].
(ii) Inhomogeneous distribution of the doping ions in the host material leading to the variation in the local concentration [35].
(iii) The transfer of excitation energy from the donor to activators [36].

In the present case, the bi-exponential fitting is related to the difference in the non-radiative probability of decays for lanthanide ions at or near the surface of the particles. Inhomogeneous distribution of the doping ions in the host material is ruled out as the lattice parameters show the quantitative substitution of co-doped ions in lattice. However, the third reason of transfer of excitation energy from donor to activator can be there in such system. Fig. 13a shows the bi-exponential fitting to 900 °C annealed 3 at.% Pb^{2+} co-doped YVO_4:$5Dy^{3+}$. The average lifetime values are found to be decreased on increasing Pb^{2+} concentration. This is due to the well known phenomenon of concentration quenching effect. The calculated average life time values for $^7F_{9/2}$ levels are 0.122, 0.104, 0.087 and 0.009 ms for 1, 3, 5 and 10 at.% Pb^{2+}

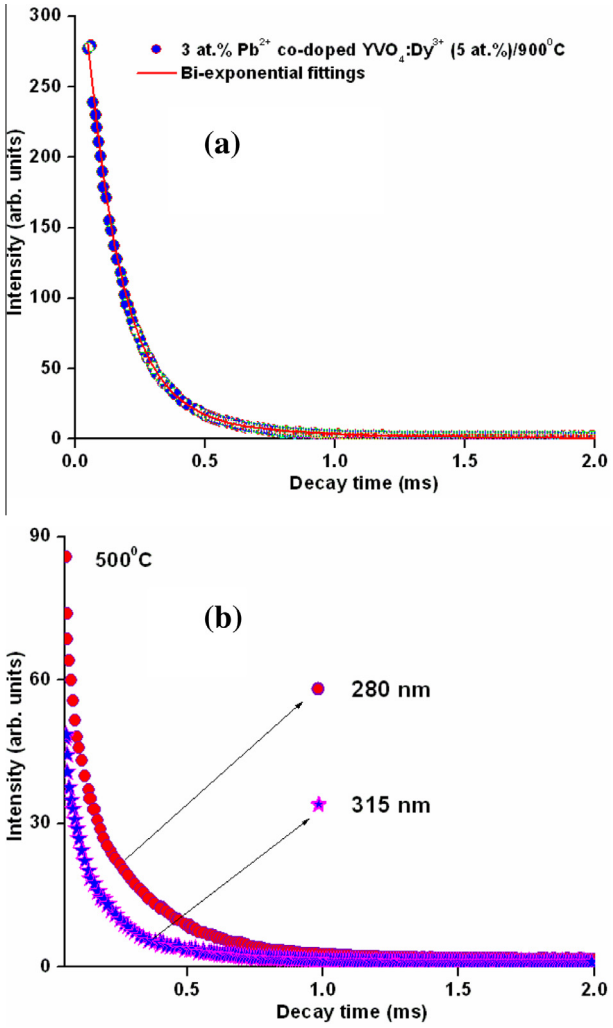

Fig. 13. (a) Bi-exponential fitting to luminescence decay data of 900 °C annealed 3 at.% Pb^{2+} co-doped YVO_4:5Dy^{3+} nanoparticles. (b) Luminescence decay spectra of 500 °C annealed 3 at.% Pb^{2+} co-doped YVO_4:5Dy^{3+} nanoparticle at 280 and 315 nm excitation.

concentration respectively under 280 nm excitation. Moreover, the lifetime value observed for 500 °C annealed 3 at.% Pb^{2+} co-doped YVO_4:5Dy^{3+} at 315 nm is shorter than that measured at 280 nm excitation (Fig. 13b). This is due to decrease in luminescence intensity at 315 nm excitation as compared to that at 280 nm excitation. Longer lifetime value or higher luminescence intensity at 280 nm excitation is related to the high population of excited photons at the $^4F_{9/2}$ level due to efficient energy transfer from Dy–O CT band to Dy^{3+}.

We see longer lifetime value in case of 500 or 900 °C annealed samples as compared to that of as-prepared samples (Figs. 11 and 12). This shows that the average lifetime increases significantly with heat treatment, which is due to decrease of non-radiative processes arising from water molecule present on the surface of nanoparticles and surface dangling bonds. Also, contribution of non-radiative relaxation from O–H is reduced with heat treatment thereby causing improvement in the size of the particles.

Determination of CIE coordinates

An important criterion for specifying the property of the phosphor is its color that can be described in terms of CIE chromaticity coordinates. So, for studying the emission color of Pb^{2+} co-doped

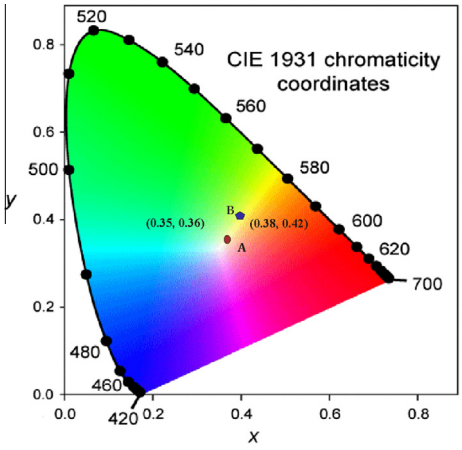

Fig. 14. CIE chromaticity of (A) as-prepared and (B) 900 °C annealed 1 at.% co-doped YVO_4:5Dy^{3+} nanoparticles under excitation wavelength at 280 nm.

YVO_4:5Dy^{3+} phosphors, we have determined the CIE coordinates of 1 at.% Pb^{2+} co-doped YVO_4:5Dy^{3+} phosphor as (0.347, 0.364), (0.362, 0.411) and (0.388, 0.424), respectively for as-prepared, 500 and 900 °C annealed sample under 280 nm excitation. And for undoped YVO_4:5Dy^{3+} phosphor CIE chromaticity lies in bluish white with CIE coordinates (0.331, 0.323) under 280 nm excitation. We see that on co-doping Pb^{2+} ions into YVO_4:5Dy^{3+} color changes from bluish white to white region on contrary to that observed on co-doping Bi^{3+} ions [31] and then shift towards yellow region as we move from 500 to 900 °C annealed sample (Fig. 14). The emission color of 900 °C annealed 7 at.% Pb^{2+} co-doped YVO_4:5Dy^{3+} phosphor under 280 nm is found to be in pure yellow region with CIE co-ordinate (0.397, 0.410). This is related to the slight increase in the value of asymmetric ratio owing to the dominance of yellow light emission over blue emission on heat treatment. This shows that annealing temperature is also responsible for tuning the color of the phosphors. We also find that the emission color remain the same even on changing the excitation wavelengths from 280 nm. However, multicolor tunable emission was accomplished by just using different excitation wavelength in Bi^{3+} co-doped YVO_4:5Dy^{3+} phosphors [31]. Under 300 nm excitation, the emission color of 1 at.% Pb^{2+} co-doped phosphor also fall in white region with CIE coordinates (0.342, 0.371) [37]. The well fitting of CIE coordinates in white region on co-doping of Pb^{2+} into YVO_4:5Dy^{3+} could serve as a good source of white light in the application of white LEDs.

Conclusions

Single tetragonal phase of YVO_4 have been prepared successfully by co-doping Pb^{2+} into YVO_4:5Dy^{3+} phosphor at comparatively low temperature of 120 °C. On annealing the samples to 900 °C the excitation spectra exhibit a broad band around 220–310 nm suggesting the efficient transfer of excitation energy from host/VO_4^{3-} to Dy^{3+}. The luminescence study show that the maximum emission intensity of Dy^{3+} is observed under 280 nm excitation and then decrease in order of 300, 315, 260 and 240 nm excitation. The optimum concentration for highest luminescent is found at 1 at.% Pb^{2+} and 7 at.% Pb^{2+} for as-prepared and 900 °C annealed samples respectively under 280 nm excitation. Both the luminescent intensity and decay lifetime increase on annealing the samples from 500 to 900 °C. The emission color of Pb^{2+} co-doped YVO_4:5Dy^{3+} fall near white region independent of excitation wavelengths. On annealing the samples to 900 °C

the emission color changes to yellow showing that the annealing temperature is also responsible for tuning of the emission color.

Acknowledgment

Ch. Victory Devi thanks Department of Chemistry, Manipur University for providing the research facilities.

Appendix A. Supplementary data

Supplementary data associated with this article can be found, in the online version, at http://dx.doi.org/10.1016/j.saa.2015.03.039.

References

[1] N. Hirosaki, R.J. Xie, K. Kimoto, T. Sekiguchi, Y. Yamamoto, T. Suehiro, M. Mitomo, Appl. Phys. Lett. 86 (2005) 211905.
[2] Z.C. Wu, J.X. Shi, J. Wang, M.L. Gong, Q. Su, J. Solid State Chem. 179 (2006) 2356.
[3] K.N. Shinde, S.J. Dhoble, A. Kumar, J. Lumin. 131 (2011) 931.
[4] P. Li, Z. Wang, Z. Yang, Q. Guo, X. Li, J. Lumin. 130 (2010) 222.
[5] Y. Liu, Z. Yang, Q. Yu, X. Li, Y. Yang, P. Li, Mater. Lett. 65 (2011) 1956.
[6] S. Nakamura, Diamond Relat. Mater. 5 (1996) 496.
[7] T. Nishida, T. Ban, N. Kobayashi, Appl. Phys. Lett. 82 (2003) 3817.
[8] T. Nishida, N. Kobayashi, Phys. Stat. Sol. (a) 176 (1999) 45.
[9] Z. Huang, Y. Chen, L. Chen, Y. Xie, L. Xiao, Y. Yang, Ceram. Int. 39 (2013) 2709.
[10] Y.-K. Kim, S. Choi, H. Jung, J. Lumin. 130 (2010) 60.
[11] C.H. Huang, T.M. Chen, Opt. Express 18 (2010) 5089.
[12] C.H. Huang, W.R. Liu, T.M. Chen, J. Phys. Chem. C 114 (2010) 18698.
[13] N. Guo, H.P. You, Y.H. Song, M. Yang, K. Liu, Y.H. Zheng, Y.J. Huang, H.J. Zhang, J. Mater. Chem. 20 (2010) 9061.
[14] Y. Wang, L. Guo, Y. Wang, J. Zhang, P. Dong, Nanoscale (2013). doi: 10.1039/C2NR33577H, accepted manuscript.
[15] L. Tian, S. Mho, J. Lumin 122–123 (2007) 99–103.
[16] M. bass, IEEE J. Quant. Electron. 11 (1975) 938.
[17] J.R. O'Connor, Appl. Phys. Lett. 9 (1996) 407.
[18] X.Z. Xio, B. Yan, J. Alloys Compd. 448 (2008) 298.
[19] J. Wu, B. Yan, J. Alloys Compd. 455 (2008) 485.
[20] X. He, L. Zhang, G. Chen, Y. Hang, J. Alloys Compd. 467 (2008) 366.
[21] J. Kucytowski, K. Wokulska, A. Kazmierczak-Balata, J. Bodzenta, T. Lukasiewicz, B. Hofman, M. Pyka, Thin Solid Films 516 (2008) 8125.
[22] P. Gerner, K. Kramer, H.U. Gudel, J. Lumin. 102–103 (2003) 112.
[23] H. Zhang, X. Fu, S. Niu, Q. Xin, J. Alloys Compd. 457 (2008) 61.
[24] M. Chen, C.G. Liu, Y.N. Liu, K.L. Huang, J. Mater. Process. Technol. 198 (2008) 129.
[25] Y.H. Wang, Y.Y. Zuo, H. Gao, Mater. Res. Bull. 41 (2006) 2147.
[26] Y.H. Zhou, J. Lin, J. Alloys Compd. 408 (2006) 856.
[27] (a) J. Lin, D.V. Sanger, M. Menning, K. Baerner, Thin Solid Films 39 (2000) 360;
(b) M.L. Pang, J. Lin, M. Yu, S.B. Wang, J. Solid State Chem. 177 (2004) 2236.
[28] M. Yu, J. Lin, J. Fang, Chem. Mater. 17 (2005) 1783.
[29] A. Kato, S. Oishi, T. Shishido, M. Yamazaki, S. Iida, J. Phys. Chem. Solids 66 (2005) 2079.
[30] A.K. Parchur, A.I. Prasad, A. Ansari, S.B. Raia, R.S. Ningthoujam, Dalton Trans. 41 (2012) 11032.
[31] Ch. Victory Devi, N. Rajmuhon Singh, J. Alloys Compd. 583 (2014) 259.
[32] N. Shanta Singh, R.S. Ningthoujam, N. Yaiphaba, S.D. Singh, R.K. Vatsa, J. Appl. Phys. 105 (2009) 064303.
[33] K. Riwotzki, M. Haase, J. Phys. Chem. B 102 (1998) 10129.
[34] M. Yu, J. Lin, Z. Zhang, J. Fu, S. Wang, H.J. Zhang, Y.C. Han, Chem. Mater. 14 (2002) 224.
[35] J.W. Stouwdam, F.C.J.M. Van Veggel, Nano Lett. 2 (2002) 733.
[36] W. Wang, M. Yu, C.K. Lin, J. Lin, J. Colloid Interf. Sci. 300 (2006) 176.
[37] S.D. Han, S.P. Khatkar, V.B. Taxak, G. Sharma, D. Kumar, Mater. Sci. Eng. B 129 (2006) 126.